



Optimizing the Design of a Hydrogen Refueling Station Integrating Renewable Energy and Seawater Desalination: A Case Study in Southern Iran

H. Maleki¹ | M.S. Spasian² | M.R. Aghamohammadi³ | M. Marzband^{4,5}

Electrical Engineering Department, Shahid Beheshti University, Tehran, Iran^{1,2,3}

Department of Electrical and Computer Engineering, Faculty of Engineering, King Abdulaziz University, Jeddah 21589, Saudi Arabia⁴

Center of Research Excellence in Renewable Energy and Power Systems, Department of Electrical and Computer Engineering, King Abdulaziz University, Jeddah 21589, Saudi Arabia⁵

Corresponding author's email: m_sepasian@sbu.ac.ir

Article Info

Article type:

Research Article

Article history:

Received: 31-December-2024

Received in revised form:
12-March-2025

Accepted: 30-March-2025

Published online: 23-Sep-2025

Keywords:

Hydrogen refueling station,
Photovoltaic,
Optimization,
Water desalination.

ABSTRACT

This study investigates the optimal design configuration of a hydrogen refueling station located in southern Iran, focusing on the integration of renewable energy sources and seawater desalination technology to achieve self-sufficiency. The station integrates various components, including photovoltaic panels, fuel cells, desalination units, natural gas and power-to-hydrogen conversion systems, and storage facilities for water and hydrogen. The primary goals are to achieve an independent power supply from renewable sources and an autonomous water supply through seawater desalination. To determine the most cost-effective configuration, a Mixed Integer Linear Programming (MILP) model is developed, taking into account the water and power consumption of each component. The objective is to minimize the Net Present Cost (NPC) of investment, maintenance, and operation. The model is implemented and solved using the CBC solver within the PYOMO environment. The study's findings reveal that converting natural gas to hydrogen is more economically viable than power-to-hydrogen conversion, with the former accounting for more than 95% of the hydrogen produced. The power demand is effectively met by combining photovoltaic systems, fuel cells, and hydrogen storage. Moreover, the study highlights the benefits of integrating water and hydrogen storage systems, which optimizes the utilization of photovoltaic energy. Excess energy generated by the photovoltaic panels is utilized for seawater desalination and the production of green hydrogen.

NOMENCLATURE

Sets

y Index of years in the project's lifetime horizon

h Index of hours in the time horizon

n Index of typical day types

C Set of HRS components

Variables

C^{IN} Investment cost of the HRS (\$)

C_y^M Annual operation cost of the HRS (\$)

C_y^R Annual replacement cost of the HRS (\$)

E_m^{H2T} The initial value of H2T(MWh)

$Q_{y,n,h}^{H2T-}$ The Charging value of H2T (MW)

$Q_{y,n,h}^{H2T+}$ The Charging value of hydrogen to H2T (MW)

$I_{y,n,h}^{H2T}$ Binary variable for the charging mode of H2T

κ_p^{P2H} Power consumption factor for P2H (MWh/ton H2)

$V_{y,n,h}^{WT}$ The charge value of WT(m3)

$W_{y,n,h}^{WT+}$ The charging value of hydrogen to WT (m3/h)

$W_{y,n,h}^{WT-}$ The charging value (m3/h)

$I_{y,n,h}^{WT}$ Binary variable for the charging mode of WT



		Parameters	
$C_{y,n,h}^{NG}$	Total natural gas cost of the HRS (\$)	K_p^{RO}	RO power consumption factor (MWh/m ³ H ₂ O)
$W_{y,n,h}^{RO}$	The water generation of the RO(m ³)	η^{FC}	Efficiency of FC
$Q_{y,n,h}^{SMR_CCS}$	The hydrogen generation of SMR_CCS (MW)	$\kappa_p^{SMR_CCS}$	SMR power consumption factor (MWh/ ton H ₂)
$P_{y,n,h}^{SMR_CCS}$	The power consumption of the SMR_CCS(MW)	$\kappa_G^{SMR_CCS}$	SMR natural gas feeding factor (m ³ / ton H ₂)
$G_{y,n,h}^{SMR_CCS}$	The natural gas consumption of the SMR_CCS (m ³)	W_{in}^{WT}	The initial value of WST(m ³)
$P_{y,n,h}^{FC}$	The electrical power generation from the FC (MW)	$\kappa_{CO_2}^{SMR_CCS}$	CO ₂ emission factor for SMR (m ³ /ton H ₂)
$Q_{y,n,h}^{FC}$	The H ₂ power consumption of the FC (MW)	$\kappa_{LHV}^{H_2}$	Lower heat value of hydrogen (MWh/ton H ₂)
$G_{y,n,h}$	The amount of gas consumed in the HRS(m ³)	η^{H_2ST}	H ₂ tank efficiency
$Q_{y,n,h}^{P2H}$	The hydrogen power generation of P2H (MW)	\overline{Q}^{-H_2T}	Charging /discharging range of the H ₂ T
$P_{y,n,h}^{P2H}$	The electrical power consumption of the P2H (MW)	\overline{W}^{-WT}	Charging /discharging range of the WT
S_c	The optimized size of the HRS components.	$R_{y,n,h}^{PV}$	The solar radiation (W/m ²)
\overline{S}^c	Maximum capacity of the HRS components		

I. Introduction

According to the International Energy Agency (IEA), the transportation sector is responsible for approximately 8 Gt CO₂ emissions, making it the third-largest carbon emitter globally [1]. Coupled with accelerated urbanization, the sector is projected to further escalate energy demand and CO₂ emissions. In 2022, global CO₂ emissions from transportation increased by over 250 Mt, reaching nearly 8 Gt CO₂. At the sector level, transportation witnessed the most significant rise in emissions, with an increase of nearly 240 Mt globally between 2022 and 2023 [2]. Thus, reducing carbon emissions from the transportation sector is an urgent challenge that must be addressed immediately. Conversely, clean hydrogen offers a promising solution for mitigating climate change and could be pivotal in the decarbonizing of transportation. Fuel cells will enable hydrogen-powered transportation to cut emissions, offering superior efficiency versus conventional engines [3]. Hydrogen production can be categorized into three primary types: gray, blue, and green hydrogen. Gray hydrogen, produced from fossil fuels without carbon capture, produces substantial carbon emissions. Carbon capture, utilization, and storage technologies are critical components in global climate change mitigation strategies, providing an effective method to substantially decrease carbon dioxide emissions from both industrial operations and energy production[4]. Blue hydrogen incorporates carbon capture and storage (CCS), which reduces its carbon footprint significantly [5]. Finally, green hydrogen is produced using renewable energy sources [6]. Grey hydrogen is currently the most economical and preferred pathway for commercial hydrogen generation [7], and green hydrogen represents only about 4% of global industrial hydrogen production [8]. Due to cost and CO₂ emission challenges, blue hydrogen is seen as a transitional solution, facilitating immediate reductions in carbon emissions [9]. Currently, blue hydrogen serves as an essential bridge between high-emission grey hydrogen and

zero-emission green hydrogen, which remains limited in scale. While the ultimate goal of the transition is prioritizing green hydrogen through electrolysis, this shift depends significantly on technological advancements in electrolysis methods. Until such breakthroughs occur, blue hydrogen provides a practical intermediate solution on the pathway to a low-carbon hydrogen economy[10] To facilitate the broader adoption of hydrogen fuel, it is essential to plan the development of hydrogen refueling stations(HRSs) and the development of hydrogen fuel in transportation and meeting various sector demands requires long-term planning for optimal production and operation of hydrogen refueling stations. A techno-economic comparison shows wind-based systems are more cost-effective than solar for green hydrogen production in Riyadh, Saudi Arabia[11]. Analysis of five European hydrogen stations shows buses average 14.62 kg per fill with 10-minute refueling times, consuming 7 kg/100 km while operating 10 hours daily with 80% availability[12]. A model for optimal siting and sizing of hydrogen refueling stations is presented to minimize consumer costs through life-cycle cost analysis and supply chain optimization[13]. In Ref. [14], a technical analysis comparing hydrogen refueling stations in Turkey and Spain demonstrates that solar systems work best for Turkey, in contrast, combined solar-wind systems are more efficient in Spain. An optimization study for Al-Kharj examines combined solar and wind technologies with storage systems, achieving efficient hydrogen production at \$9.34/kg LCOH[15]. A novel optimization study in Datong analyzes hybrid renewable systems with hydrogen refueling, demonstrating the effective integration of solar power and storage solutions[16]. A techno-economic analysis of a wind-PV hybrid hydrogen station in Çeşme, Turkey demonstrates the feasibility of fueling 25 vehicles daily, with hydrogen production costs ranging from \$7.53-7.87/kg using HOMER software[17]. A comparative analysis of three PV-based hydrogen production methods reveals that grid-

connected systems achieve the lowest costs (5.5 €/kg), outperforming standalone systems with batteries (5.74 €/kg) and fuel cells (7.38 €/kg)[18]. This study optimizes a hydrogen refueling station combining PV and electrolyzer, showing trade-offs between CO₂ reduction and system capacity utilization while maintaining high operational efficiency[19]. According to research [20], a Moroccan study evaluates solar-powered hydrogen stations for taxis, showing cost reductions with increased capacity.

This study reveals renewable facilities combining photovoltaic storage deliver optimal economics, achieving production expenses of 4.78-5.55 €/kg for clean vehicle support[21]. In Ref.[22], a study on 1GW agrivoltaic systems across five countries demonstrated the feasibility of combining solar power with agriculture for hydrogen production. Their analysis showed that such systems could support millions of hydrogen vehicle refueling annually while maintaining agricultural productivity, with hydrogen production costs ranging from £3.06 to £6.38/kg depending on location. The integrated energy approach can optimize hydrogen production while supporting the simultaneous generation of clean electricity, heat, and cooling which is essential for decarbonizing the energy sector [23].

Discovering enhanced methods to utilize eco-friendly renewable energy sources has become highly significant, as these approaches can mitigate the detrimental impacts of carbon dioxide emissions that threaten our ecosystem, which is already facing concerning levels of climate change[24]. The rise of Power-to-Gas technology signals an innovative breakthrough in energy conversion and storage systems, presenting a hopeful solution for managing renewable energy inconsistency while advancing decarbonization efforts throughout the energy landscape. P2G functions by transforming surplus electricity production into hydrogen-based fuels through electrolytic processes[25]. According to Ref. [26], Research shows that among integrated renewable systems, biomass achieves the highest exergy efficiency while geothermal offers the best economic performance for hydrogen production via electrolysis.

Ref. [27] presents a comprehensive methodology for dimensioning components of an on-site hydrogen refueling station. The system's electrical requirements are fulfilled through a grid-connected photovoltaic array. Considering the intermittent nature of solar resources, the conventional electrical grid provides supplementary power during periods of insufficient generation while also accommodating the export of excess production. Ref. [28] illuminates the prospects for green hydrogen development in Tunisia through a rigorous economic analysis. The study presents a comprehensive assessment of the levelized hydrogen cost and net profit metrics for a photovoltaic-powered hydrogen refueling station, offering a detailed evaluation and discussion of the financial implications. In [29] a novel off-grid integrated energy system structure was proposed to

address both market hydrogen demands and the electrical, heating, and cooling requirements of the HRS support building. Through a cost-minimizing mixed integer quadratic constrained programming model, researchers solved optimal sizing and scheduling challenges, with results demonstrating the structure's effectiveness and advantages, as documented.

In [30], an integrated energy system combining wind turbines with an on-site hydrogen refueling station is proposed that can simultaneously satisfy cooling, heating, power, and hydrogen demands. The system determines equipment capacity while optimizing total annual costs. Configurations with varying numbers of wind turbines were analyzed. When equipped with 5 turbines, the system achieves 91% hydrogen self-production with minimal energy redundancy. Ref. [31] analyzes three system configurations: standalone wind park hydrogen refueling stations with battery backup, fuel cell backup, and grid connection. The analysis considers local wind potential, equipment costs, and hydrogen demand. The research aims to determine the optimal sizing for wind turbines, electrolyzers, power converters, and storage tanks. Ref. [32] introduces an off-grid integrated electricity-hydrogen system that incorporates solar and hydroelectric renewable energy sources, serves both industrial and residential loads, and includes electric vehicle charging infrastructure, hydrogen refueling for fuel cell vehicles, natural gas pipeline integration, and seasonal hydrogen storage capabilities. According to [33], an optimized hybrid renewable energy system with a vanadium redox flow battery for on-site hydrogen production was evaluated for serving 20 fuel cell vehicles across seven South Korean locations. Their analysis reveals levelized hydrogen costs ranging from 8.77-19.1 \$/kg and energy costs between 2.1-4.58 \$/kWh. The global community faces a crisis as water resources become increasingly scarce and water stress intensifies, necessitating the development of innovative and environmentally friendly technologies to ensure a reliable and sustainable water supply for future generations. The nexus of water and energy systems means that water scarcity can significantly impact the efficiency and reliability of power generation[34]. Moreover, hydrogen production through both natural gas reforming and electricity-to-hydrogen conversion needs substantial water consumption as a feedstock, and expanding these facilities without considering water supply could further intensify water stress. On the one hand, reverse osmosis technology for seawater desalination has proven to be a promising solution to water scarcity. However, one of the key challenges in implementing desalination is public concern over energy consumption[35] and its expansion requires the development of electrical energy production to meet the significant power demands of these facilities.

TABLE 1 provides a summary of recent scientific research related to previous perspectives on hydrogen refueling

stations. Additionally, this table highlights the unique aspects of the present study in comparison to previous research. After reviewing the literature on hydrogen refueling stations, several advantages and limitations become apparent. Most studies [21, 27-33] successfully integrate renewable energy sources with hydrogen production for transportation, demonstrating technical feasibility across different geographical contexts.

TABLE 1 COMPARISON OF THIS STUDY WITH THE LITERATURE REVIEW

Ref.	Year	RES	FC	P2H	H2T	SMR-CCS	RO-WT	HRS Water usage
[27]	2020	✓	✗	✓	✓	✗	✗	✗
[28]	2022	✓	✗	✓	✓	✗	✗	✗
[29]	2022	✓	✗	✓	✓	✗	✗	✗
[21]	2023	✓	✓	✓	✓	✗	✗	✗
[30]	2023	✓	✗	✓	✓	✗	✗	✗
[31]	2023	✓	✓	✓	✓	✗	✗	✗
[32]	2024	✓	✓	✓	✓	✗	✗	✗
[33]	2024	✓	✗	✓	✓	✗	✗	✗
This paper	2025	✓	✓	✓	✓	✓	✓	✓

However, these works primarily focus on green hydrogen production through electrolysis without considering blue hydrogen alternatives.

A significant limitation in the existing literature is the lack of attention to water requirements for hydrogen production. None of the reviewed studies [21, 27-33] address water usage or incorporate water desalination in HRS, which is crucial for sustainable operation, especially in water-scarce regions. Additionally, while some studies incorporate energy storage solutions and fuel cells, they typically don't optimize for multiple energy carriers simultaneously.

The current paper addresses these gaps by integrating both blue hydrogen and green hydrogen production pathways, incorporating water desalination technology, explicitly accounting for water consumption in hydrogen production, and representing a more comprehensive approach to hydrogen refueling station design and optimization. In summary, the innovations of this paper include the following:

A. Renewable Power and Water Supply for HRS: Providing an optimal solution for the power and water supply of HRS in remote and water-stressed areas, integrating photovoltaic energy, seawater desalination, fuel cell, and storage technologies.

B. Optimal Hydrogen Production Method for HRS: Analyzing the economics of green hydrogen production through water electrolysis and blue hydrogen through methane reforming with carbon capture technology, considering investment costs, natural gas, electricity, and water consumption.

C. Maximization of Photovoltaic Energy Usage: Optimizing surplus photovoltaic energy utilization for green hydrogen production and seawater desalination and storage systems.

This study addresses the optimal design of a hydrogen refueling station by integrating photovoltaic (PV) as a renewable energy source, power to hydrogen(P2H), steam methane reformer equipped by carbon capture (SMR-CCS), fuel cell (FC), seawater desalination (RO), and water and hydrogen storage units (WT & H2T), with focusing on meeting the power and water requirement for hydrogen production in a self-sufficient manner through photovoltaic and seawater desalination. The mathematical model is formulated based on Mixed-Integer Linear Programming (MILP). By selecting a suitable geographical area in southern Iran for station development, historical radiation and temperature data have been examined. Finally, the optimization problem was solved in the PYOMO environment using the CBC solver.

II. The structure of the proposed HRS

The Fig.1, illustrates the schematic diagram of the integrated on-site Hydrogen Refueling Station. The system consists of several components: PV, FC, P2H, SMR-CCS, RO, WT, and H2T. The HRS is connected to the natural gas network. This configuration efficiently integrates diverse energy conversion and storage elements to meet hydrogen demand. Hydrogen is produced through the P2H and SMR-CCS, while the PV and FC provide the necessary power for the HRS. The RO desalinates seawater to supply fresh water for hydrogen production. The sizing and operation of all components are optimized to minimize the net present cost (NPC) of the project.

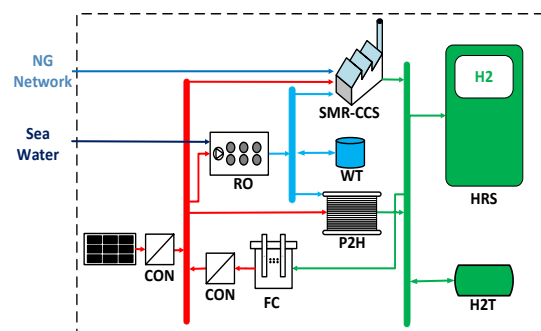


Fig. 1. The schematic of the proposed HRS

III. Mathematical formulation

This paper determines the optimal capacity of the HRS by minimizing the overall project cost, as presented in Eq. (1). In this context, Lf refers to the project's lifetime, and Nn indicates the number of representative days considered. To make the problem more manageable and solvable, the typical days (Nd) are selected according to seasonal periods. The real interest rate (r) is defined in equation (2), where Z and I correspond to the nominal interest rate and annual inflation, respectively.

Minimise : (1)

$$NPC = (C^{IN} + \sum_{y=1}^{Lf} (C_y^M + C_y^R) / (1+r)^y +$$

$$\sum_{y=1}^{Lf} \sum_{n=1}^{Nd} \sum_{h=1}^{24} N_n C_{y,n,h}^{NG} / (1+r)^y)$$

$$r = \frac{Z - I}{1 + I} \quad (2)$$

The investment, operational, and replacement costs of the HRS components are calculated based on their optimal capacities, as defined in equations (3) to (5).

$$C^{IN} = \sum_{c \in C} \lambda_c^I S_c \quad (3)$$

$$C_y^M = \sum_{c \in C} \lambda_c^M S_c \quad \forall 1 \leq y \leq Lf \quad (4)$$

$$C_y^R = \sum_{c \in C} \lambda_{c,y}^R S_c \quad \forall 1 \leq y \leq Lf \quad (5)$$

The variable S is associated with the optimal size of the energy HRS components. The parameters λ_c^I , λ_c^M and $\lambda_{c,y}^R$ correspond to the unit costs for investment, operation, and replacement of the HRS components. The replacement factor is only applied to equipment with a shorter useful life than the project's duration, and its value remains zero throughout the equipment's lifespan. When the equipment reaches the end of its useful life, the replacement cost is incurred in the relevant year. The set C refers to the HRS components. Natural gas sourced from the network is utilized in the steam methane reformers to generate hydrogen. The hourly cost of purchasing gas from the network is calculated in equation (6). The parameter $G_{y,n,h}$ represents the quantity of gas purchased per hour, while the other parameter λ^G is associated with the gas price.

$$C_{y,n,h}^{NG} = \lambda^G G_{y,n,h} \quad (6)$$

A. P2H model

The P2H is capable of converting electricity into hydrogen. The mathematical model for the P2H system is formulated based on the relationship between the electricity input and hydrogen output, as shown in Eq. (7). The electrolyzer consumes approximately 55 kW of electrical energy to produce one kilogram of hydrogen at 60% efficiency[36, 37]. Furthermore, Eq. (8) determines the

water consumption of the P2H, which is based on the volume of hydrogen produced

$$P_{y,n,h}^{P2H} = k_P^{P2H} Q_{y,n,h}^{P2H} \quad (7)$$

$$W_{y,n,h}^{P2H} = k_W^{P2H} Q_{y,n,h}^{P2H} \quad (8)$$

B. RO model

At present, reverse osmosis using membrane technology is the most widely employed method for seawater desalination. This process requires electrical energy for desalination and is more energy-efficient compared to other methods [38]. In [39], A review of data from over 70 seawater desalination plants reveals that the lowest specific energy consumption for reverse osmosis (RO), considering the plant's additional electrical consumption, is 3.1 kWh/m³.

$$P_{y,n,h}^{RO} = SEC^{RO} W_{y,n,h}^{RO} \quad (9)$$

The parameters $P_{y,n,h}^{RO}$, SEC^{RO} and $W_{y,n,h}^{RO}$ represent, in order, the electrical energy usage in kWh, the volume of freshwater produced in cubic meters, and the specific energy consumption coefficient of the RO plant.

C. FC model

The proposed HRS focuses on utilizing carbon-free power generation systems. Considering the unavailability of the PV at night and its reliance on weather conditions, the FC serves as a controllable energy source. Thus, since electricity can be generated from hydrogen via an FC, this unit is included in the study as described in equation (10).

$$P_{y,n,h}^{FC} = \eta^{FC} Q_{y,n,h}^{FC} \quad (10)$$

D. SMR-CCS

The SMR is a widely used method for hydrogen production, accounting for approximately 76% of global hydrogen production. It is also important to note that hydrogen production from coal gasification represents 22%, while only 2% of global hydrogen production comes from electrolysis[40].

Hydrogen production from natural gas requires the consumption of natural gas, electricity, and water, and results in CO₂ emissions. The necessary heat is produced by burning natural gas, while electrical energy is used to set up the required process conditions. In this study, the mathematical model for this unit is developed using equations (11) to (13).

$$P_{y,n,h}^{SMR-CCS} = K_P^{SMR-CCS} Q_{y,n,h}^{SMR-CCS} \quad (11)$$

$$G_{y,n,h}^{SMR-CCS} = K_G^{SMR-CCS} Q_{y,n,h}^{SMR-CCS} \quad (12)$$

$$W_{y,n,h}^{SMR-CCS} = K_W^{SMR-CCS} Q_{y,n,h}^{SMR-CCS} \quad (13)$$

The parameters $Q_{y,n,h}^{SMR-CCS}$, $K_P^{SMR-CCS}$, and $K_G^{SMR-CCS}$ represent the hydrogen production rate in kW, the electricity consumption coefficients, and gas consumption coefficients per kW of hydrogen produced. In[41], The natural gas feed consumption for the SMR is reported to be 3.5 kg of natural

gas per kg of hydrogen produced. The steam methane reformer can be integrated with a carbon capture system, which significantly lowers carbon emissions. However, this setup increases the consumption of methane gas and electricity, depending on the carbon capture level. In this study, a carbon capture rate of 85% is assumed.

E. H2T

In the proposed HRS the hydrogen tank is also considered, and the (14)-(19) related to this component, the hourly stored energy of tank ($E_{y,n,h}^{H2T}$) is updated by (14). According to (15) – (17) and using binary variables ($I_{y,n,h}^{H2T+}$ & $I_{y,n,h}^{H2T-}$), this system can be used in charging ($Q_{y,n,h}^{H2T+}$) or discharging ($Q_{y,n,h}^{H2T-}$) modes. According to (18) the amount of hydrogen stored in the first hour ($E_{y,n,1}^{H2T}$) is the same as the 24th hour ($E_{y,n,24}^{H2T}$). In addition, the amount of initial charge of the tank is also defined as a variable (E_{in}^{H2T}) and its amount will be optimized by (19):

$$E_{y,n,h}^{H2T} = E_{y,n,h-1}^{H2T} + \kappa_{LHV}^{H2} (Q_{y,n,h}^{H2T+} - Q_{y,n,h}^{H2T-}) \quad (14)$$

$$Q_{y,n,h}^{H2T+} \leq I_{y,n,h}^{H2T+} \bar{Q}^{H2T} \quad (15)$$

$$Q_{y,n,h}^{H2T-} \leq I_{y,n,h}^{H2T-} \bar{Q}^{H2T} \quad (16)$$

$$I_{y,n,h}^{H2T+} + I_{y,n,h}^{H2T-} \leq 1 \quad (17)$$

$$E_{y,n,24}^{H2T} = E_{y,n,1}^{H2T} \quad (18)$$

$$E_{y,n,0}^{H2T} = E_{in}^{H2T} \quad (19)$$

The κ_{LHV}^{H2} is related to the lower heat value of hydrogen.

F. WT

The mathematical model of the water storage tank is expressed in (20)- (25). The hourly stored water in the tank ($V_{y,n,h}^{WT}$) is updated by (20) and the WT can be used in charging($Q_{y,n,h}^{WT+}$) or discharging($Q_{y,n,h}^{WT-}$) mode by (21)-(23). According to (24) the amount of water stored in the first hour is the same as the 24th hour. In addition, the amount of initial charge of the tank is also defined as a variable and its value is optimized by (25).

$$V_{y,n,h}^{WT} = V_{y,n,h-1}^{WT} + W_{y,n,h}^{WT+} - W_{y,n,h}^{WT-} \quad (20)$$

$$W_{y,n,h}^{WT+} \leq I_{y,n,h}^{WT+} \bar{W}^{WT} \quad (21)$$

$$W_{y,n,h}^{WT-} \leq I_{y,n,h}^{WT-} \bar{W}^{WT} \quad (22)$$

$$I_{y,n,h}^{WT+} + I_{y,n,h}^{WT-} \leq 1 \quad (23)$$

$$V_{y,n,24}^{WT} = V_{y,n,1}^{WT} \quad (24)$$

$$V_{y,n,0}^{WT} = V_{in}^{WT} \quad (25)$$

G. balance constraints

The balance constraints for electricity, water, hydrogen, and natural gas demands and supplies in the HRS are expressed in (26)- (29), respectively. The electrical energy balance is defined by (26), the water balance by (27), and the

hydrogen balance by (28). Finally, (29) balances the import of gas and its consumption in the SMRs.

$$P_{n,s,h}^D = P_{n,s,h}^{PV} + P_{n,s,h}^{FC} - P_{n,s,h}^{P2H} - P_{n,s,h}^{SMR-CCS} - P_{n,s,h}^{RO} \quad (26)$$

$$W_{n,s,h}^D = W_{n,s,h}^{RO} - W_{n,s,h}^{P2H} - W_{n,s,h}^{SMR-CCS} - Q_{n,s,h}^{WT+} + Q_{n,s,h}^{WT-} \quad (27)$$

$$Q_{n,s,h}^D = Q_{n,s,h}^{P2H} + Q_{n,s,h}^{SMR-CCS} - Q_{n,s,h}^{FC} - Q_{n,s,h}^{H2T+} + Q_{n,s,h}^{H2T-} \quad (28)$$

$$G_{n,s,h} = G_{n,s,h}^{SMR-CCS} \quad (29)$$

H. PV

According to Eq. (30), the amount of power generation from PV depends on the amount of radiation and the temperature of the environment [42, 43].

$$P_{y,n,h}^{PV} = S_{pv} \times \frac{R_{y,n,h}^{PV}}{R_{ref}^{PV}} \times \left[1 - N_T \left(T_{y,n,h}^{PV} + \frac{NOCT - 20}{800} R_{y,n,h}^{PV} - T_{ref}^{PV} \right) \right] \quad (30)$$

The PV power in this model represents the total power of the PV unit at the maximum power point. Also, S_{pv} shows the nominal power of the optimal size for the PV unit at the maximum power point and the standard condition of $R_{ref}^{PV} = 1000W / m^2$ and $T_{ref}^{PV} = 25^\circ C$ N_T and NOCT respectively show the power temperature coefficient at the maximum power point and nominal operating cell temperature.

IV. Solution method

In this model, the mathematical formulation is presented to minimize investment, operation, and emission costs. The problem is solved using the CBC solver within the PYOMO software package, which supports MILP formulations. PYOMO is an open-source software package based on Python that offers a wide range of optimization capabilities for formulating, solving, and analyzing optimization models [30].

The proposed on-site HRS integrates solar energy, natural gas, and seawater desalination technologies. This study considers the optimal HRS design in Gankhak-e Sheykhi, Bushehr province, Iran. This area benefits from abundant solar and natural gas resources, as illustrated in Fig. 2, and is close to seawater. Historical data on solar radiation and temperature for this region, spanning 22 years, has been sourced from NASA. Irradiance and temperature seasonal averages for typical days have been calculated, as shown in Fig. 3 and Fig. 4.

The HRS is engineered to address specific demands for electricity, water, and hydrogen. In addition to the fixed demands it must fulfill, the HRS components also have variable electricity and gas consumption, which are accounted for in the energy supply and demand balance. Basic design parameters, including energy prices, investment, operational and replacement costs, technical specifications, and parameters for each component, are detailed in Tables 2 to 5.

In this study, the HRS is designed to supply the average hydrogen load of 3200 kg/day, sufficient to refuel 100 trucks, each equipped with a 32 kg hydrogen tank. As shown in Fig.5, during the night, hydrogen demand decreases and reaches its minimum between 24:00 to 7:00. Conversely, during the day, the hydrogen demand increases, peaking between 16:00 to 18:00. Electrical demand of the on-site HRS encompasses both industrial and non-industrial consumptions. It should be mentioned that industrial electrical consumption pertains to the energy required for HRS operations, calculated hourly using mathematical models. According to Fig. 5 the assumed electrical load profile, non-industrial electrical consumption, related to non-industrial buildings such as ventilation and lighting electricity consumption is minimized during the night, specifically from 23:00 to 07:00. During the day, electricity consumption rises due to the activation of welfare services and increased cooling requirements, peaking between 11:00 to 17:00.



Fig. 2. Selected study area: Gankhak-e Sheykhi, Bushehr Province

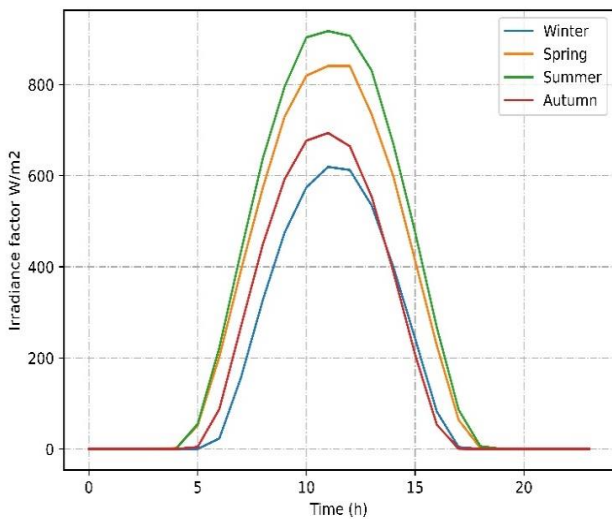


Fig. 3. Seasonal average irradiance

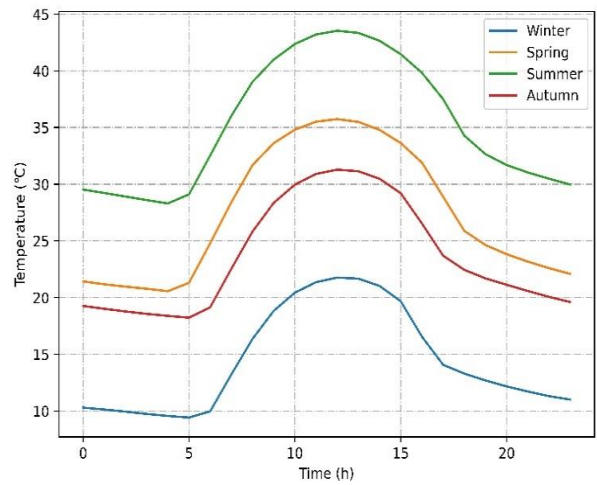


Fig. 4. Seasonal average temperature

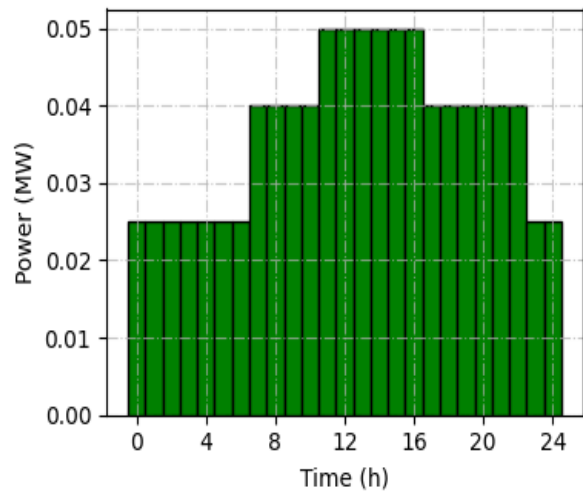
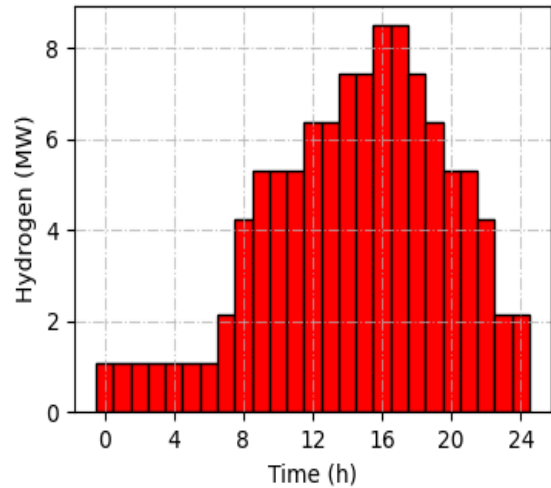


Fig. 5. Hydrogen and Electrical demand of the HRS

TABLE 2 HRS COMPONENTS COST DATA

Item	C ^I	C ^M	C ^R	Lf
PV	1000 \$/kW	10 \$/kW/year	0	25
FC	1000 \$/kW	0	-	500
P2H	872 \$/kW	19.2 \$/kW/year	50	15
SMR_CCS	1583 \$/kW	47.5 \$/kW/year	0	25
CON	200 \$/kW	5 \$/kW/year	0	25
H2T	700 \$/kg	0	-	200
RO	50.8 \$/m ³ /h	0.29 \$/m ³ /year	0	30
WT	311 \$/m ³ /h	31 \$/m ³ /year	0	30

TABLE 3 HRS BASIC DATA

Item	Value	Unit
lifetime	25	year
Interest rate	8	%
Inflation rate	2	%
Annual operation days	336	day
Natural gas price	0.3	\$/m ³

TABLE 4 THE COEFFICIENT [44, 45]

Component	k^P [kWh/kg H ₂]	k^G [kg/kg H ₂]	k^W [m ³ /kgH ₂]
P2H	55	0	0.009
SMR_CCS	4.42	3.4	0.0097

TABLE 5 THE COMPONENT PARAMETERS [39, 46, 47]

Component	Parameters
RO	$SEC = 3.1 kWh / m^3$
PV	$R_{ref}^{PV} = 1000W / m^2$ $T_{ref}^{PV} = 25^\circ C$ $N_T = -0.45 \% / ^\circ C$ $NOCT = 45^\circ C$

V. Results and discussion

The optimal capacities of the on-site HRS components and the cost breakdown of the project are detailed in Tables 6 and 6. For hydrogen production components: 1- The optimal sizes are 7.76 MW for the SMR-CCS and 0.14 MW for the P2H. 2- The optimal capacity for the H2T is 297 kg. Comparing the capacities, it is evident that the P2H has a relatively minor role compared to the SMR-CCS, with the P2H capacity being less than 2% of the total. The energy

storage capacity in the H2T, considering the LHV of hydrogen at 33.3 kWh/kg and an assumed operational limit of 90 %, total 8.9 MWh. Regarding the electricity production components: 1-The optimal sizes are 1.34 MW for the PV and 0.82 MW for the FC. 2- The PV system is notably larger compared to FC. For water supply, an RO with a capacity of 7 m³ and a WT with a capacity of 25 m³ are optimal for meeting the water requirements of the HRS. These optimal sizes ensure the efficient operation and cost-effectiveness of the HRS in meeting hydrogen, electricity, and water demands.

TABLE 6 THE HRS COEFFICIENT OPTIMAL SIZING

Components	Unit	Value
PV	MW	1.34
FC	MW	0.82
CON	MW	2.16
P2H	MW	0.14
SMR-CCS	MW	7.76
H2T	kg	297
RO	m ³	7
WT	m ³	25

According to the results shown in Table 7, the net present cost of this project for the optimal scheme is \$53.13 billion, encompassing installation, repair, and operational expenses. The cost breakdown is as follows: investment costs (\$15.22 million), maintenance costs (\$5.12 million), replacement costs (\$0.95 million), and natural gas purchase costs (\$31.84 million). As illustrated in Fig. 6, the most significant portion of the HRS cost is attributed to natural gas expenses (60% of the total cost). The investment cost (IC), maintenance cost (MC), and replacement cost (RC) are replacement costs follow, with a share of 28.9%, 9.6 %, and 1.8%, respectively.

TABLE 7 THE COST BREAKDOWN OF OPTIMAL HRS

Cost component	Value(M\$)
IC	15.22
MC	5.12
RC	0.95
NGC	31.84
NPC	53.13

VI. Optimal operation of the HRS

Figures 7 -9 illustrate the hourly electrical, hydrogen, and water balances in the on-site HRS for the first year, across each season.

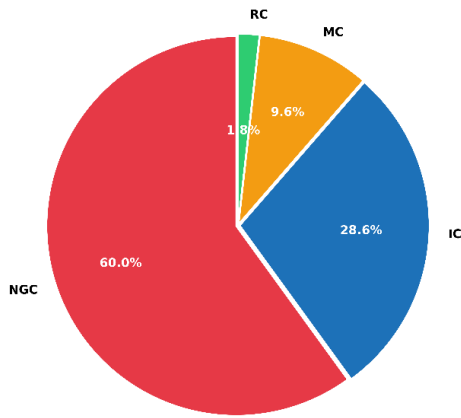


Fig. 6. Percentage of on-site HRS project costs in different sectors

According to Fig. 7, it is evident that the electricity during the day is primarily supplied by the PV system, with its output varying by season. In summer, the PV system reaches its peak output of 1.03 MW at noon, while in winter, the maximum production decreases to 0.79 MW. Conversely, the FC operates as a controllable source, balancing the electrical power when PV output fluctuates. During daylight hours, the FC's power decreases and may even be inactive during specific periods: 8:00 AM- 3:00 PM in spring, 8:00 AM-4:00 PM in summer, 10:00 AM- 2:00 PM in autumn, and 10:00 AM- 2:00 PM in winter. At night, when solar energy is unavailable, the FC supplies the entire electrical power needed for the on-site HRS. Additionally, the power consumption for the HRS components is depicted. The SMR-CCS, which plays a significant role in hydrogen production, is the largest electricity consumer in the HRS. In the proposed HRS the maximum available power from the PV system is utilized and any surplus electricity generated is used to produce hydrogen through the P2H during the day.

The role of the on-site HRS components in hydrogen balancing is illustrated in Fig. 8. In the current structure of the on-site HRS, both the SMR-CCS and P2H contribute to hydrogen production. However, the optimal results show that most of the hydrogen required is produced by the SMR-CCS across all seasons. Fig. 8 reveals that, for most of the 24-hour cycle, the SMR-CCS meets the hydrogen demand, with the P2H's contribution being minimal. Additionally, a 40% minimum production limit for the SMR-CCS results in surplus hydrogen being stored in the H2T between 22:00 and 07:00, when demand falls below this production threshold. This stored hydrogen is discharged during the day, although the discharge period varies slightly across seasons. In summer and spring, the P2H's higher participation at noon requires the H2T to release some of its stored energy in the morning to accommodate the P2H's energy needs.

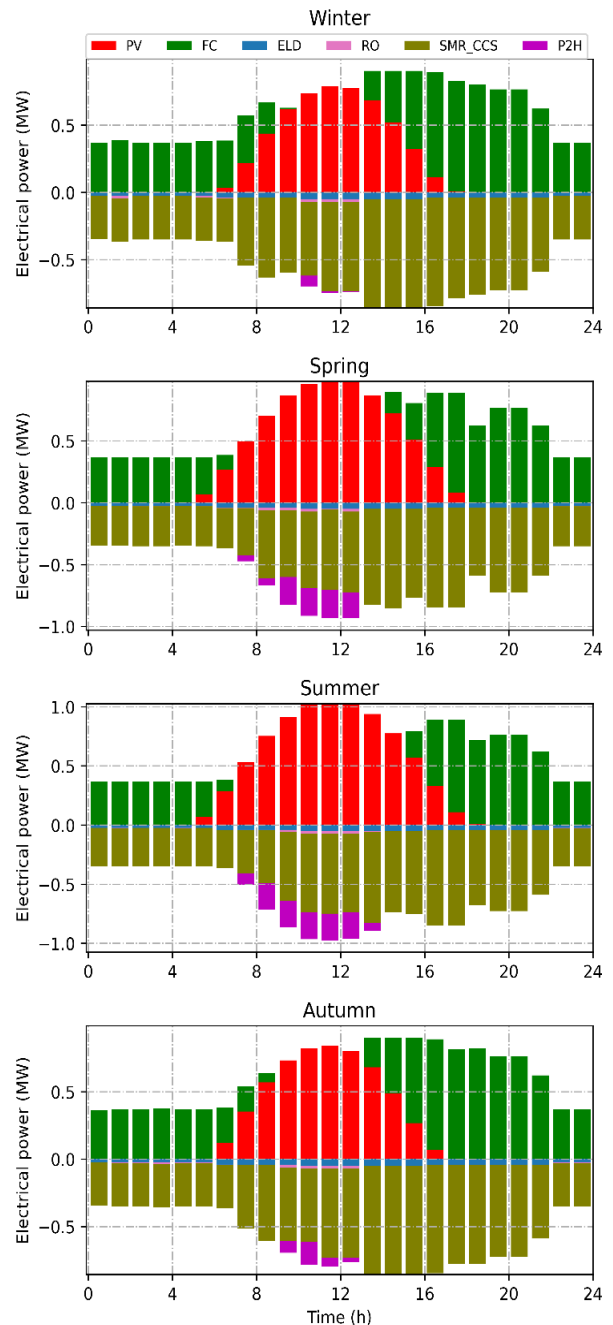


Fig. 7. Electrical power balance in various seasons

In this study, the water required for hydrogen production in the on-site HRS is supplied by an optimized reverse osmosis (RO) unit and a water tank. The RO unit desalinates seawater using electrical power. Fig. 9 shows the water balance within the on-site HRS. This unit operates predominantly during the day when solar energy is abundant. The RO's peak operation occurs between 11:00 and 14:00 in all seasons except winter. In winter, the RO operates between 11:00 and 14:00.

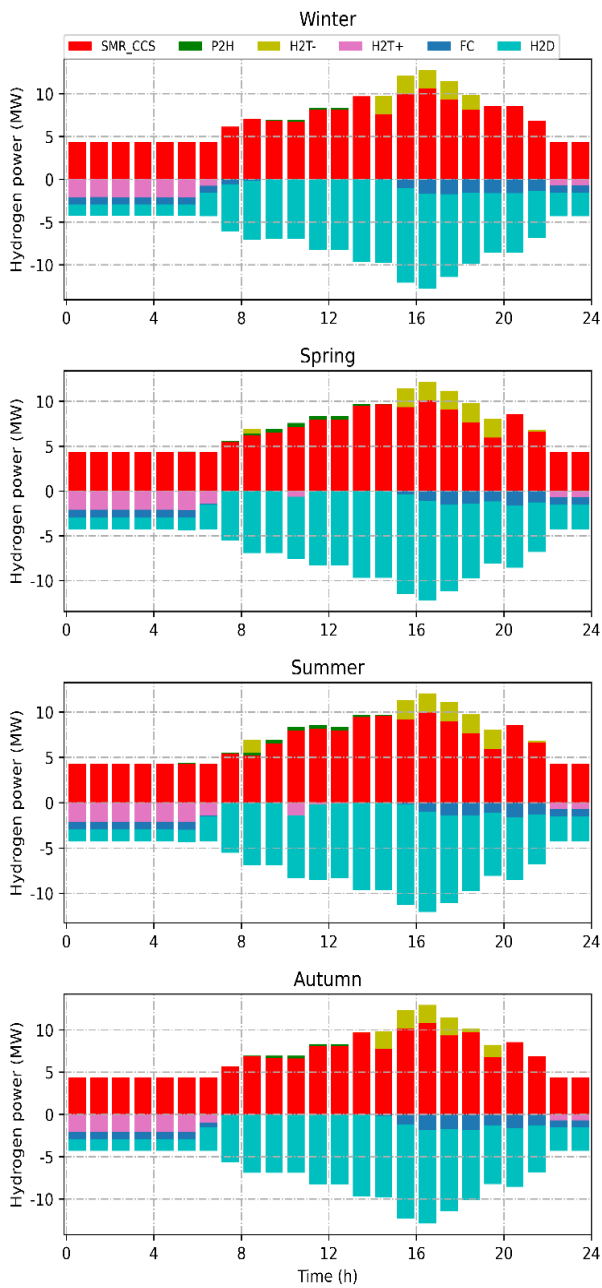


Fig. 8. Hydrogen power balance in various seasons

The RO is generally inactive between 14:00 and 23:00 across all seasons except summer. During summer, due to increased electricity production from PV in the afternoon, some of the surplus electricity is used by the RO, allowing it to operate until 15:00. During this period, the water tank is adequately filled and used during the night. Additionally, since the operating hours of the RO in winter and autumn are shorter compared to other seasons, it is necessary to utilize it more during the night to balance water production and consumption. In winter, the RO is reactivated from 23:00 to 08:00, with its utilization optimized throughout these hours. Conversely, the RO's utilization is lowest during these hours in summer.

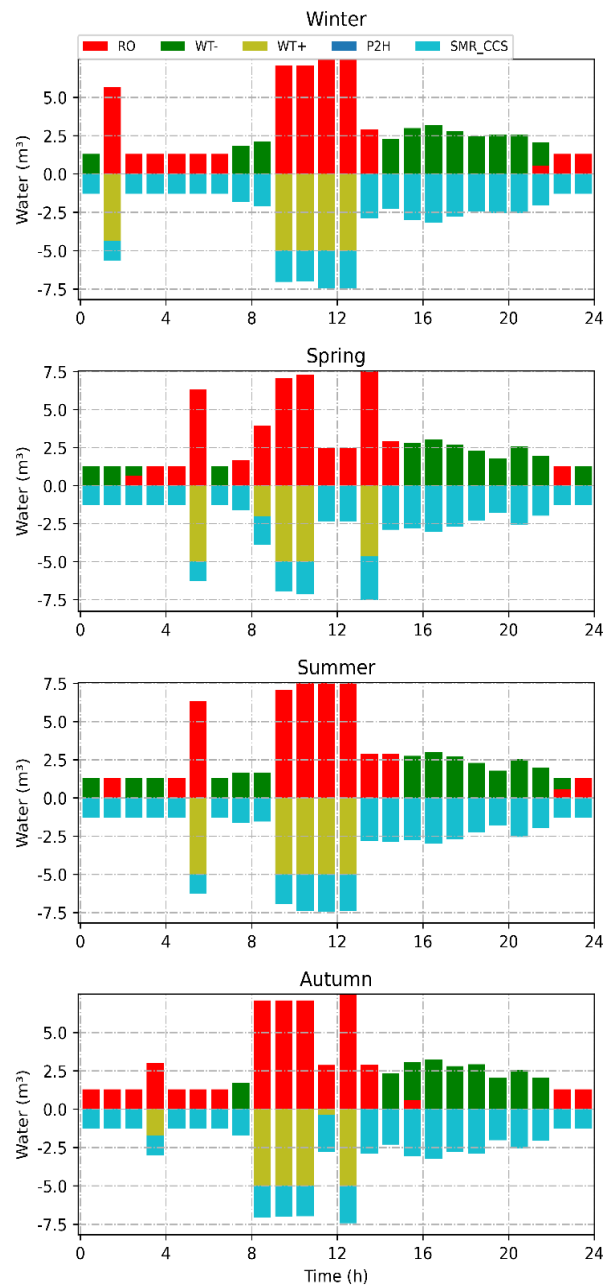


Fig. 9. Water balance in various seasons

VII. The Levelized Cost of Hydrogen

The Levelized Cost of Hydrogen (LCOH) metric quantifies the ratio of NPC to cumulative hydrogen production throughout the HRS's lifespan. The LCOH will be determined using (31).

$$LCOH = \frac{NPC}{\sum_{y=1}^{L_f} \sum_{n=1}^{N_d} \sum_{h=1}^{24} Q_{y,n,h}^D / (1+r)^y} \tag{31}$$

In order to validate our research outcomes, we compared our results with established literature as presented in Table 8. This table chronicles the evolution of hydrogen production

economics through various Power-to-Hydrogen (P2H) implementations from 2020 to 2025. Our hybrid system, combining P2H with SMR-CCS, achieves a remarkable LCOH of \$3.82/kg. This economic performance demonstrates a substantial advantage when contrasted with previous research efforts. Contemporary studies published in 2024 reported significantly higher production costs, with values ranging from \$8.77-\$19.1[33] and \$11.36 [48]. Similarly, projections for 2025 technologies in earlier research anticipated costs between \$13.81-\$17.52 [49], while studies from 2020-2023 documented LCOH figures between \$5.17 and \$13.55 [21, 27, 31, 49]. The marked cost reduction achieved in our research can be attributed to the novel integration approach that leverages complementary strengths of both P2H and SMR-CCS technologies. This strategic combination optimizes resource utilization and operational efficiency, yielding a cost structure that substantially improves upon single-technology solutions. The economic advantage demonstrated here suggests promising pathways toward commercially viable low-carbon hydrogen production.

TABLE 8 LCOH in Recent Literature

REF.	YEAR	HYDROGEN PRODUCTION METHOD	LCOH [\$/KG]
[27]	2020	P2H	8.96-13.55
[50]	2020	P2H	5.51*-6.12*
[21]	2023	P2H	5.17*-6*
[31]	2023	P2H	6.75*
[33]	2024	P2H	8.77-19.1
[48]	2024	P2H	11.36*
[49]	2025	P2H	13.81*-17.52*
THIS PAPER	2025	P2H & SMR-CCS	3.76

*Values were converted from Euro to US Dollar using the annual average exchange rates: 1.1410 (2020), 1.0817 (2023), and 1.0820 (2024) as reported by the Federal Reserve Economic Data (FRED, Series *AEXUSEU*)[51] using the monthly average exchange rates: 1.0356 (Jan 2025) as reported by the Federal Reserve Economic Data (FRED, Series *EXUSEU*)[52]

VIII. Sensitivity analysis

This section presents a comprehensive sensitivity analysis of the hydrogen production system's economic performance metrics net present cost and levelized cost of hydrogen concerning six key parameters: natural gas price, investment costs, project lifetime, interest rate, and solar radiation. The analysis evaluates how variations in these parameters within a $\pm 10\%$ range affect the system's economic viability.

I. Parameter Impact on NPC

Figure 10 illustrates how changes in key parameters within a $\pm 10\%$ range affect the NPC. Natural gas price shows the most significant impact with a strong linear relationship, where a 10% increase results in approximately 12.5% higher costs from 56.3 to 62.5 million dollars, demonstrating the substantial contribution of fuel expenses to the system's economics. Interest rate displays an inverse relationship to NPC, where a 10% increase reduces costs by about 8% from 56.3 to 51.8 million dollars, reflecting how financing conditions significantly impact long-term project economics. Investment costs and project lifetime show moderate influences with similar positive slopes, indicating that higher capital costs or longer project durations both increase overall system costs proportionally. Solar Radiation exhibits an almost horizontal line with a slight negative slope, indicating minimal impact on NPC across the variation range. This stability suggests that the system design effectively mitigates potential economic risks associated with solar resource variability, making the proposed hybrid hydrogen production system resilient to fluctuations in renewable energy availability.

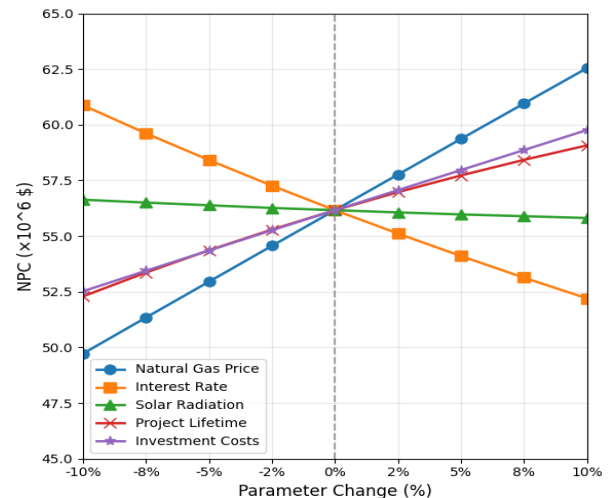


Fig. 10. Impact of varying parameters on the NPC

J. Parameter Impact on LCOH

Figure 11 illustrates how changes in key parameters within a $\pm 10\%$ range affect the LCOH. Natural gas price demonstrates the most significant influence, showing a strong linear relationship where a 10% increase raises LCOH from 4.02 to 4.50 \$/kg while a 10% decrease reduces it to 3.58 \$/kg. This substantial impact highlights the critical role of fuel costs in hydrogen production economics. Investment costs follow with moderate influence, showing a positive correlation where increased capital expenditure directly increases production costs. Project lifetime displays an inverse relationship to LCOH, with longer durations reducing unit costs as capital expenses are distributed over more production years. Interest rate shows a modest positive

correlation with LCOH, indicating that financing conditions affect production costs but less dramatically than fuel prices. Solar radiation exhibits minimal influence with an almost horizontal trend line, confirming the system's economic resilience to solar energy variability. This stability represents a valuable characteristic of the hybrid hydrogen production system, particularly in regions with seasonal weather patterns.

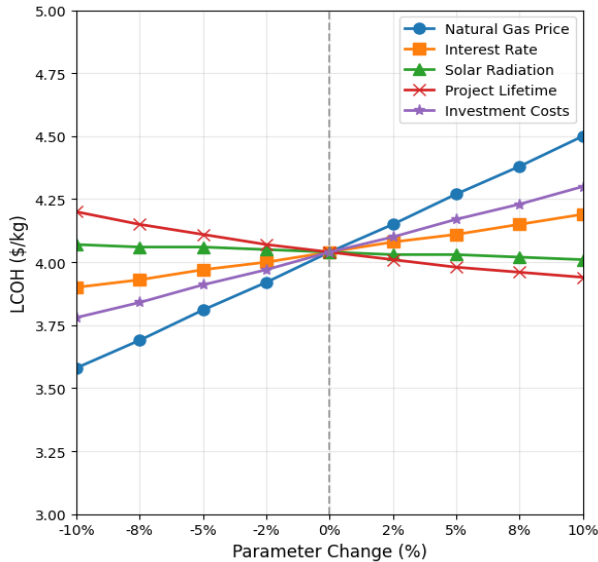


Fig. 11. Impact of varying parameters on the LCOH

IX. Practical Significance of Research

Findings

To ensure the practical applicability of this research's results, the following aspects have been considered in both the mathematical modeling and the case study:

a) Considering that both hydrogen production pathways require multiple inputs, this research's mathematical modeling has comprehensively addressed resource requirements. For blue hydrogen production through SMR-CCS, the model accounts for methane gas as the main feedstock along with electricity and water consumption. Similarly, for green hydrogen production, both electricity and water requirements are incorporated in the P2H modeling. To ensure the HRS's self-sufficiency and avoid placing demands on existing infrastructure, the research includes optimal sizing and operation of seawater desalination with water storage capabilities. The electricity consumption of all processes, including desalination, has been included in the comprehensive modeling approach.

b) The HRS location in southern Iran was strategically selected to ensure reliable access to its three essential inputs: natural gas, seawater, and renewable resources. This coastal positioning guarantees uninterrupted resource availability throughout the planning horizon. To maximize renewable energy utilization, the specific site was chosen within high-potential photovoltaic areas identified by the SATBA

organization in Bushehr province[53]. The design ensures complete independence in electricity supply through optimal sizing of solar components, informed by a comprehensive analysis of 22 years of historical NASA weather data. This integrated approach to site selection and renewable energy system design creates a self-sufficient hydrogen production facility with secure resource access.

Given the considerations mentioned above and based on the optimal sizing obtained for components, it is evident that implementing blue hydrogen within the planned horizon will be more optimal than green hydrogen. Research comparisons confirm that our hybrid blue-green hydrogen model achieves lower production costs than green hydrogen alternatives. Furthermore, the development of both production pathways enhances resource delivery security for hydrogen refueling stations, addressing a critical requirement for reliable hydrogen supply infrastructure.

X. Conclusion

This study presents a comprehensive approach for developing low-carbon hydrogen refueling stations with integrated water management. Key findings include:

Sustainable Water and Power Supply: The research optimizes both water and power provision through an integrated systems approach. For power management, the study incorporates photovoltaics, fuel cells, and hydrogen storage with precisely modeled component requirements. For water supply, the system includes seawater desalination and water storage facilities specifically designed to meet the substantial water demands of hydrogen production via electrolysis, ensuring a sustainable and independent water supply chain. This comprehensive approach to resource management creates a self-sufficient system capable of reliable hydrogen production without dependence on external water or power infrastructure.

Cost-Competitive Hydrogen Production: Analysis of investment, maintenance, and operational costs reveals natural gas-based hydrogen production with carbon capture remains economically dominant, comprising over 95% of the required capacity compared to electrolysis. Our hybrid system achieves an LCOH of \$3.82/kg, substantially lower than comparable studies reporting costs between \$5.17-\$19.1/kg. This economic advantage demonstrates how strategic integration of complementary technologies improves cost efficiency.

Optimized Resource Management and System Flexibility: The integration of water desalination, storage systems, and power-to-hydrogen conversion achieves maximum renewable energy utilization by directing surplus photovoltaic energy to water treatment and green hydrogen production. This integrated approach enhances overall system flexibility, with the combination of reverse osmosis and water storage reducing optimal RO capacity by 15%.

Robust System Design: Sensitivity analysis confirms the system's remarkable resilience to parameter variations. Natural gas price shows the most impact on economics, while solar radiation exhibits minimal influence, indicating the system effectively mitigates risks associated with renewable resource variability. This stability ensures reliable performance across changing conditions.

Future work will explore the impact of PV system optimization through tracking systems to maximize solar energy capture. The research will also evaluate alternative energy management strategies and their influence on hybrid energy system design and performance. These enhancements aim to further improve system efficiency and reduce costs as electrolysis technology advances, supporting the transitional pathway from blue to green hydrogen production while maintaining consistent resource delivery security.

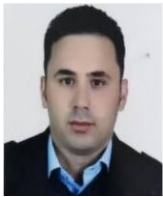
REFERENCES

- [1] IEA, "CO2 Emissions in 2022," IEA, 2023. [Online]. Available: <https://iea.blob.core.windows.net/assets/3c8fa115-35c4-4474-b237-1b00424c8844/CO2Emissionsin2022.pdf>
- [2] IEA, "CO2 Emissions in 2023," 2024. [Online]. Available: <https://iea.blob.core.windows.net/assets/33e2badc-b839-4c18-84ce-f6387b3c008f/CO2Emissionsin2023.pdf>
- [3] E. Monteiro and P. S. D. Brito, "Hydrogen supply chain: Current status and prospects," *Energy Storage*, vol. 5, no. 7, p. e466, 2023, doi: 10.1002/est.2.466.
- [4] E. Hanson, C. Nwakile, and V. O. Hammed, "Carbon capture, utilization, and storage (CCUS) technologies: Evaluating the effectiveness of advanced CCUS solutions for reducing CO2 emissions," *Results in Surfaces and Interfaces*, vol. 18, p. 100381, 2025/01/01/ 2025, doi: 10.1016/j.rsurfi.2024.100381.
- [5] A. Ajanovic, M. Sayer, and R. Haas, "The economics and the environmental benignity of different colors of hydrogen," *International Journal of Hydrogen Energy*, vol. 47, no. 57, pp. 24136-24154, 2022/07/05/ 2022, doi: 10.1016/j.ijhydene.2022.02.094.
- [6] Q. Hassan, S. Algburi, A. Z. Sameen, H. M. Salman, and M. Jaszczur, "Green hydrogen: A pathway to a sustainable energy future," *International Journal of Hydrogen Energy*, vol. 50, pp. 310-333, 2024/01/02/ 2024, doi: 10.1016/j.ijhydene.2023.08.321.
- [7] M. H. Ali Khan, R. Daiyan, P. Neal, N. Haque, I. MacGill, and R. Amal, "A framework for assessing economics of blue hydrogen production from steam methane reforming using carbon capture storage & utilisation," *International Journal of Hydrogen Energy*, vol. 46, no. 44, pp. 22685-22706, 2021/06/28/ 2021, doi: 10.1016/j.ijhydene.2021.04.104.
- [8] S. Shiva Kumar and H. Lim, "An overview of water electrolysis technologies for green hydrogen production," *Energy Reports*, vol. 8, pp. 13793-13813, 2022/11/01/ 2022, doi: 10.1016/j.egy.2022.10.127.
- [9] O. Massarweh, M. Al-khuzaei, M. Al-Shafi, Y. Bicer, and A. S. Abushaikh, "Blue hydrogen production from natural gas reservoirs: A review of application and feasibility," *Journal of CO2 Utilization*, vol. 70, p. 102438, 2023/04/01/ 2023, doi: 10.1016/j.jcou.2023.102438.
- [10] F. S. AlHumaidan, M. Absi Halabi, M. S. Rana, and M. Vinoba, "Blue hydrogen: Current status and future technologies," *Energy Conversion and Management*, vol. 283, p. 116840, 2023/05/01/ 2023, doi: 10.1016/j.enconman.2023.116840.
- [11] I. B. Mansir, P. C. Okonkwo, and N. Farouk, "Technoeconomic Optimization of a Photovoltaic Wind Energy-Based Hydrogen Refueling Station: A Case Study," *Energy Technology*, vol. 11, no. 7, p. 2201490, 2023, doi: 10.1002/ente.202201490.
- [12] R. Caponi, A. Monforti Ferrario, L. Del Zotto, and E. Bocci, "Hydrogen refueling stations and fuel cell buses four year operational analysis under real-world conditions," *International Journal of Hydrogen Energy*, vol. 48, no. 54, pp. 20957-20970, 2023/06/29/ 2023, doi: 10.1016/j.ijhydene.2022.10.093.
- [13] H. Sun, C. He, X. Yu, M. Wu, and Y. Ling, "Optimal siting and sizing of hydrogen refueling stations considering distributed hydrogen production and cost reduction for regional consumers," *International Journal of Energy Research*, vol. 43, no. 9, pp. 4184-4200, 2019, doi: 10.1002/er.4544.
- [14] M. Gökçek et al., "Optimum sizing of hybrid renewable power systems for on-site hydrogen refuelling stations: Case studies from Türkiye and Spain," *International Journal of Hydrogen Energy*, vol. 59, pp. 715-729, 2024/03/15/ 2024, doi: 10.1016/j.ijhydene.2024.02.068.
- [15] P. C. Okonkwo et al., "Utilization of renewable hybrid energy for refueling station in Al-Kharj, Saudi Arabia," *International Journal of Hydrogen Energy*, vol. 47, no. 53, pp. 22273-22284, 2022/06/26/ 2022, doi: 10.1016/j.ijhydene.2022.05.040.
- [16] J. He, Y. Wu, M. Wu, M. Xu, and F. Liu, "Two-stage configuration optimization of a novel standalone renewable integrated energy system coupled with hydrogen refueling," *Energy Conversion and Management*, vol. 251, p. 114953, 2022/01/01/ 2022, doi: 10.1016/j.enconman.2021.114953.
- [17] M. Gökçek and C. Kale, "Techno-economical evaluation of a hydrogen refuelling station powered by Wind-PV hybrid power system: A case study for İzmir-Çeşme," *International Journal of Hydrogen Energy*, vol. 43, no. 23, pp. 10615-10625, 2018/06/07/ 2018, doi: 10.1016/j.ijhydene.2018.01.082.
- [18] E. M. Barhoumi, P. C. Okonkwo, I. Ben Belgacem, M. Zghaibeh, and I. Tlili, "Optimal sizing of photovoltaic systems based green hydrogen refueling stations case study Oman," *International Journal of Hydrogen Energy*, vol. 47, no. 75, pp. 31964-31973, 2022/09/01/ 2022, doi: 10.1016/j.ijhydene.2022.07.140.
- [19] H. Aki, I. Sugimoto, T. Sugai, M. Toda, M. Kobayashi, and M. Ishida, "Optimal operation of a photovoltaic generation-powered hydrogen production system at a hydrogen refueling station," *International Journal of Hydrogen Energy*, vol. 43, no. 32, pp. 14892-14904, 2018/08/09/ 2018, doi: 10.1016/j.ijhydene.2018.06.077.
- [20] S. Bahou, "Techno-economic assessment of a hydrogen refuelling station powered by an on-grid photovoltaic solar system: A case study in Morocco," *International Journal of Hydrogen Energy*, vol. 48, no. 61, pp. 23363-23372, 2023/07/19/ 2023, doi: 10.1016/j.ijhydene.2023.03.220.
- [21] E. M. Barhoumi, "Optimal design of standalone hybrid solar-wind energy systems for hydrogen-refueling station Case study," *Journal of Energy Storage*, vol. 74, p. 109546, 2023/12/25/ 2023, doi: 10.1016/j.est.2023.109546.
- [22] J. Baker, M. Guler, A. Medonna, Z. Li, and A. Ghosh, "Analysis of large-scale (1GW) off-grid agrivoltaic solar farm for hydrogen-powered fuel cell electric vehicle

- (HFCEV) charging station," *Energy Conversion and Management*, vol. 323, p. 119184, 2025/01/01/ 2025, doi: 10.1016/j.enconman.2024.119184.
- [23] N. Li, X. Zhao, X. Shi, Z. Pei, H. Mu, and F. Taghizadeh-Hesary, "Integrated energy systems with CCHP and hydrogen supply: A new outlet for curtailed wind power," *Applied Energy*, vol. 303, p. 117619, 2021/12/01/ 2021, doi: 10.1016/j.apenergy.2021.117619.
- [24] A. Riki, M. Oukati Sadegh, and O. Narouei, "Flexibility-Constrained Energy Management of Smart Energy Hubs Considering Peer to Peer Transactive Energy and Demand Response Program," *International Journal of Industrial Electronics Control and Optimization*, vol. 8, no. 1, pp. 67-82, 2025, doi: 10.22111/ieco.2024.49216.1587.
- [25] M. Feili and M. T. Aameli, "The P2P Energy Management Scheme for Integrated Energy Microgrid Considering P2G and Electricity Network Fee," *International Journal of Industrial Electronics Control and Optimization*, vol. 8, no. 1, pp. 1-23, 2025, doi: 10.22111/ieco.2024.49044.1583.
- [26] M. Zoghi, N. Hosseinzadeh, S. Gharaie, and A. Zare, "4E comprehensive comparison and optimization of different renewable power sources for green hydrogen production," *Renewable Energy*, vol. 240, p. 122254, 2025/02/15/ 2025, doi: 10.1016/j.renene.2024.122254.
- [27] R. P. Micena, O. R. Llerena-Pizarro, T. M. de Souza, and J. L. Silveira, "Solar-powered Hydrogen Refueling Stations: A techno-economic analysis," *International Journal of Hydrogen Energy*, vol. 45, no. 3, pp. 2308-2318, 2020/01/13/ 2020, doi: 10.1016/j.ijhydene.2019.11.092.
- [28] E. M. Barhoumi *et al.*, "Techno-economic analysis of photovoltaic-hydrogen refueling station case study: A transport company Tunis-Tunisia," *International Journal of Hydrogen Energy*, vol. 47, no. 58, pp. 24523-24532, 2022/07/08/ 2022, doi: 10.1016/j.ijhydene.2021.10.111.
- [29] Y. Pang, L. Pan, J. Zhang, J. Chen, Y. Dong, and H. Sun, "Integrated sizing and scheduling of an off-grid integrated energy system for an isolated renewable energy hydrogen refueling station," *Applied Energy*, vol. 323, p. 119573, 2022/10/01/ 2022, doi: 10.1016/j.apenergy.2022.119573.
- [30] X. Zhao, H. Mu, N. Li, X. Shi, C. Chen, and H. Wang, "Optimization and analysis of an integrated energy system based on wind power utilization and on-site hydrogen refueling station," *International Journal of Hydrogen Energy*, vol. 48, no. 57, pp. 21531-21543, 2023/07/05/ 2023, doi: 10.1016/j.ijhydene.2023.03.056.
- [31] E. M. Barhoumi *et al.*, "Techno-economic optimization of wind energy based hydrogen refueling station case study Salalah city Oman," *International Journal of Hydrogen Energy*, vol. 48, no. 26, pp. 9529-9539, 2023/03/26/ 2023, doi: 10.1016/j.ijhydene.2022.12.148.
- [32] R. Hemmati, S. M. Bornapour, and H. Saboori, "Standalone hybrid power-hydrogen system incorporating daily-seasonal green hydrogen storage and hydrogen refueling station," *Energy*, vol. 295, p. 131122, 2024/05/15/ 2024, doi: 10.1016/j.energy.2024.131122.
- [33] Y. Choi and S. Bhakta, "Hybrid solar photovoltaic-wind turbine system for on-site hydrogen production: A techno-economic feasibility analysis of hydrogen refueling Station in South Korea's climatic conditions," *International Journal of Hydrogen Energy*, vol. 93, pp. 736-752, 2024/12/03/ 2024, doi: 10.1016/j.ijhydene.2024.11.037.
- [34] Y. Wang, Z. Zhou, G. Betrie, K. Zhang, and E. Yan, "Power generation-cooling water Nexus: Impacts of cooling water shortage on power system operation - a simulation case study in Illinois, U.S.," *Applied Energy*, vol. 377, p. 124440, 2025/01/01/ 2025, doi: 10.1016/j.apenergy.2024.124440.
- [35] H. Shemer, S. Wald, and R. Semiat, "Challenges and Solutions for Global Water Scarcity," *Membranes*, vol. 13, no. 6, p. 612, 2023, doi: 10.3390/membranes13060612.
- [36] K. Bareiß, C. de la Rua, M. Möckl, and T. Hamacher, "Life cycle assessment of hydrogen from proton exchange membrane water electrolysis in future energy systems," *Applied Energy*, vol. 237, pp. 862-872, 2019, doi: 10.1016/j.apenergy.2019.01.001.
- [37] X. Shi, X. Liao, and Y. Li, "Quantification of fresh water consumption and scarcity footprints of hydrogen from water electrolysis: A methodology framework," *Renewable Energy*, vol. 154, pp. 786-796, 2020/07/01/ 2020, doi: 10.1016/j.renene.2020.03.026.
- [38] H. Mehrjerdi, "Modeling and integration of water desalination units in thermal unit commitment considering energy and water storage," *Desalination*, vol. 483, p. 114411, 2020, doi: 10.1016/j.desal.2020.114411.
- [39] J. Kim, K. Park, D. R. Yang, and S. Hong, "A comprehensive review of energy consumption of seawater reverse osmosis desalination plants," *Applied Energy*, vol. 254, p. 113652, 2019, doi: 10.1016/j.apenergy.2019.113652.
- [40] "Enabling a low-carbon economy," in "Hydrogen Strategy," U.S. DEPARTMENT OF ENERGY, 2020. [Online]. Available: https://www.energy.gov/sites/prod/files/2020/07/f76/USD_OE_FE_Hydrogen_Strategy_July2020.pdf
- [41] E. Cetinkaya, I. Dincer, and G. F. Naterer, "Life cycle assessment of various hydrogen production methods," *International Journal of Hydrogen Energy*, vol. 37, no. 3, pp. 2071-2080, 2012/02/01/ 2012, doi: 10.1016/j.ijhydene.2011.10.064.
- [42] J. Karkhaneh, Y. Allahviridizadeh, H. Shayanfar, and S. Galvani, "Risk-constrained probabilistic optimal scheduling of FCPP-CHP based energy hub considering demand-side resources," *International Journal of Hydrogen Energy*, vol. 45, no. 33, pp. 16751-16772, 2020, doi: 10.1016/j.ijhydene.2020.04.131.
- [43] Y. Riffonneau, S. Bacha, F. Barruel, and S. Ploix, "Optimal power flow management for grid connected PV systems with batteries," *IEEE Transactions on sustainable energy*, vol. 2, no. 3, pp. 309-320, 2011, doi: 10.1109/TSTE.2011.2114901.
- [44] M. Katebah, M. m. Al-Rawashdeh, and P. Linke, "Analysis of hydrogen production costs in Steam-Methane Reforming considering integration with electrolysis and CO2 capture," *Cleaner Engineering and Technology*, vol. 10, p. 100552, 2022/10/01/ 2022, doi: 10.1016/j.clet.2022.100552.
- [45] A. O. Oni, K. Anaya, T. Giwa, G. Di Lullo, and A. Kumar, "Comparative assessment of blue hydrogen from steam methane reforming, autothermal reforming, and natural gas decomposition technologies for natural gas-producing regions," *Energy Conversion and Management*, vol. 254, p. 115245, 2022/02/15/ 2022, doi: 10.1016/j.enconman.2022.115245.
- [46] Y. Allahviridizadeh, H. Shayanfar, and M. P. Moghaddam, "Stochastic expansion planning of transmission system and energy hubs in the presence of correlated uncertain variables," *IET Generation, Transmission & Distribution*, vol. 17, no. 4, pp. 911-946, 2023, doi: 10.1049/gtd2.12715.
- [47] F. A. Kassab, B. Celik, F. Locment, M. Sechilariu, S. Liaquat, and T. M. Hansen, "Optimal sizing and energy management of a microgrid: A joint MILP approach for

minimization of energy cost and carbon emission," *Renewable Energy*, vol. 224, p. 120186, 2024/04/01/ 2024, doi: 10.1016/j.renene.2024.120186.

- [48] R. Caponi, E. Bocci, and L. Del Zotto, "On-site hydrogen refuelling station techno-economic model for a fleet of fuel cell buses," *International Journal of Hydrogen Energy*, vol. 71, pp. 691-700, 2024/06/19/ 2024, doi: 10.1016/j.ijhydene.2024.05.216.
- [49] N. Wolf, R. Neuber, A. Mädlow, and M. Höck, "Techno-economic analysis of green hydrogen supply for a hydrogen refueling station in Germany," *International Journal of Hydrogen Energy*, vol. 106, pp. 318-333, 2025/03/06/ 2025, doi: 10.1016/j.ijhydene.2025.01.424.
- [50] P. K. Rose and F. Neumann, "Hydrogen refueling station networks for heavy-duty vehicles in future power systems," *Transportation Research Part D: Transport and Environment*, vol. 83, p. 102358, 2020/06/01/ 2020, doi: 10.1016/j.trd.2020.102358.
- [51] B. o. G. o. t. F. R. S. (US). U.S. Dollars to Euro Spot Exchange Rate [AEXUSEU] [Online] Available: <https://fred.stlouisfed.org/series/AEXUSEU>
- [52] B. o. G. o. t. F. R. S. (US). U.S. Dollars to Euro Spot Exchange Rate [EXUSEU] [Online] Available: <https://fred.stlouisfed.org/series/EXUSEU>
- [53] [Online]. Available: https://www.satba.gov.ir/suna_content/media/image/2021/01/8717_orig.pdf



Hamed Maleki received MS degree at SBU University, Iran, 2012. He is currently pursuing his PhD's degree in electrical engineering from Shahid Beheshti University, Tehran. His research interest's energy hub optimization, planning, hydrogen and low-carbon dispatch in power systems.



Mohammad Sadegh Sepasian received the B.Sc. degree from Tabriz University (Iran) in 1990 and the M.Sc. and Ph.D. degrees from Tehran University and Tarbiat Modares University (Iran) in 1993 and 1999, respectively. Since 1994, he has been with Abbaspour Technical and Engineering Department, Shahid Beheshti University in Tehran, Iran

where he is currently an associate professor. He managed several national projects for the Iranian power grid. His research interests are distribution networks, power system planning, electric vehicles, and smart grids.



Mohammad Reza Aghamohammadi was born in Iran on August 5, 1955. He received his BSC degree from Sharif University of Technology 1985, MSc degree from Manchester University (UMIST) in 1989 and his PhD from Tohoku University, Japan in 1994. He is professor of the electrical engineering department and head of Iran Dynamic

Research Center. His research interest includes application of artificial intelligent techniques and non-model based approaches for dynamic security assessment and enhancement of power systems.



Mousa Marzband (SMIEEE17) is a distinguished academic and Fellow of the Higher Education Academy, recognized for his pioneering contributions to electrical engineering and clean energy systems. With over 140 publications in top-tier journals, his research has garnered more than 11,700 citations and an h-index of 61. His global

influence has been acknowledged by Thomson Reuters, ranking him among the top 1% of researchers (2019–2021), and by Stanford University, listing him among the top 2% worldwide (2022–2023). Prof. Marzband has successfully secured over £2.5 million in research funding from prestigious organizations, including Innovate UK, EPSRC (UK), the Qatar National Research Fund, and the Marie Skłodowska-Curie Actions (EU). His funded projects span a wide range of industrial and academic applications, from offshore wind power systems in the UK to green hydrogen development in Azerbaijan and capacity allocation studies in Australia and the UK. With 14 years of academic leadership and over eight years of industrial experience, Prof. Marzband bridges the gap between research and real-world implementation. His expertise lies in renewable energy integration, power systems, and grid resilience, driving advancements in sustainable energy solutions and e-mobility. Through global collaborations, he continues to shape the future of energy systems, accelerating the transition toward a net-zero future.